Proceedings of the ASME 2013 International Design Engineering Technical Conferences and Computers and Information in Engineering Conference
IDETC/CIE 2013
August 4-7, 2013, Portland, Oregon, USA

DETC2013-13101

A THREE-DIMENSIONAL MUSCULOSKELETAL DRIVER MODEL TO STUDY STEERING TASKS

Naser Mehrabi*
Department of Systems Design Engineering
University of Waterloo
Waterloo, Ontario, Canada
Email: nmehrabi@uwaterloo.ca

Reza Sharif Razavian
John McPhee
Department of Systems Design Engineering
University of Waterloo Waterloo, Ontario, Canada
{rsharifr, mcphee}@uwaterloo.ca

ABSTRACT

Realistic driver models can play an important role in developing new driver assistance technologies. A realistic driver model can reduce the time-consuming trial and error process of designing and testing products, and thereby reduce the vehicle's development time and cost. A realistic model should provide both driver path planning and arm motions that are physiologically possible. The interaction between a driver's hand and steering wheel can influence control performance and steering feel.

The aim of this work is to develop a comprehensive yet practical model of the driver and vehicle. Consequently, a neuromuscular driver model in conjunction with a high-fidelity vehicle model is developed to learn and understand more about the driver's performance and preferences, and their effect on vehicle control and stability. This driver model can provide insights into task performance and energy consumption of the driver, including fatigue and co-contraction dynamics of a steering task. In addition, this driver model in conjunction with a high-fidelity steering model can be used to develop new steering technologies such as Electric Power Steering.

INTRODUCTION

The steering system is the major part of a vehicle with which the driver interacts. For better comfort and stability, many assistive systems (e.g. electric power steering, EPS) have been developed. These technologies aim to aid the drivers in performing driving tasks, and to improve the *steering feel*.

To better design a steering system, the driver's characteristics must be considered. However, developing driver-based technologies requires proper understanding of the driver. Unfortunately, our understanding of driver's behavior is still insufficient, especially in interaction with the steering system. The goal of this paper is to present a physics-based simulation framework for further study of driver/vehicle interactions – a tool that can expedite the development process of steering systems by eliminating the need for trial-and-error iterations.

So far, the majority of research on human steering systems has considered a path-following driver model [1]. In such models, the physiological characteristics and limitations of the driver are usually neglected. A minority of research papers have followed a different approach and focused on the human musculoskeletal system, which gives insight into task performance, disturbance rejection and energy consumption. For example, Pick and Cole in a series of papers [2]- [5] introduced a comprehensive neuromuscular system (NMS) model structure, and studied the effect of steering torque feedback and driver learning behavior. Later in [6], the authors identified the torque-generating muscles in a steering maneuver task by measuring the muscle activation using electromyography (EMG) techniques.

In this research, a model predictive controller (MPC) has been used as the path-following controller (to represent the vision-based decision making of the brain) [7]. The output of the MPC controller, the prediction of the required steering wheel angle, is then used to find the joint torques in the driver's arm,

*Address all correspondence to this author.

and later to identify the muscle forces required for the maneuver.

The controller is coupled to a 3D musculoskeletal arm model, which closely resembles a human arm; however, the unimportant degrees of freedom for a steering task, such as internal/external rotation of the shoulder joint, and the corresponding muscles are removed. Moreover, neural feedback, e.g. stretch reflex, is included in the driver model to enhance our understanding of disturbance rejection and precision control in human limbs.

Using this musculoskeletal framework, we can predict muscle loads, which can be used to quantify objective criteria such as fatigue and muscle co-contraction for drivers of different age, gender, and physical ability, thereby supporting the development of new steering technologies such as EPS and lane-keeping.

DYNAMICAL MODELING

To obtain reliable results, both the driver and the vehicle should be accurately modeled. Modeling error in each part will affect the behavior of the other, and interpretation of the data will be obscured. In the following sections, the driver and the vehicle models are presented.

3D Arm Model

Even though two dimensional musculoskeletal models can provide useful insight into dynamical behavior of a muscle activated arm, the range of motion is essentially limited [8] [9]. Therefore, for higher fidelity, and to study broader ranges of steering wheel rotation, a three-dimensional arm model has to be employed.

Fig. 1 shows the schematic of developed arm. The number of degrees of freedom in this model is smaller than the actual degrees of freedom in a human arm. Unlike the human arm, this model does not allow supination/pronation of the forearm, nor does it allow the internal/external rotation of the shoulder. These degrees of freedom have negligible effect on the kinematics of the steering act for the range of steering angle ($\pm 40^\circ$) considered here; moreover, the associated muscles (Supinator, Pronator Teres, Subscapularis and Infraspinatus) have negligible activation (at most 5% for Infraspinatus) during steering [10]. Such simplifications reduce the complexity of the model, while maintaining the versatility of the model.

In this 3D arm model, the shoulder and the elbow joints are modeled, respectively, as a universal joint and a revolute joint. The wrist joint is modeled as a spherical joint, and the hand is assumed to be fixed to the steering wheel. The schematic of the developed arm model is shown in Fig. 1.

As can be seen in Fig. 1, the arm model consists of four links: the body (shoulder), the upper arm (Humerus), the forearm (Ulna and Radius) and the hand. The universal joint connects the Humerus to the shoulder, while the revolute joint attaches the Ulna and Radius to the Humerus. Since the supination or pronation is neglected in this model, the twisting of Ulna and Radius is not modeled. As a result, the two bones form a rigid structure. The unactuated spherical joint at the wrist connects the hand to Ulna/Radius Finally, the hand is fixed to the steering wheel, to reduce the complexity. The arm/steering wheel model is, therefore, a one-degree-of-freedom (DoF) mechanism, and the steering wheel angle will fully define all the joint angles.

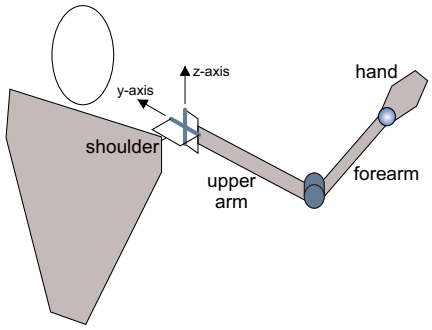

FIGURE 1. SCHEMATIC VIEW OF THE 3D ARM

In total, 11 muscles are used in this model to move the arm (see Fig. 2). The rest of the muscles that are removed are either negligible in effect (e.g. Anconeus), or related to the removed degrees of freedom (e.g. supination). Moreover, in spite of significant activity of some wrist actuator muscles during steering [10], the wrist joint is left unactuated because the elbow and shoulder muscles are of the most interest here. The muscle parameters used in this work are taken from [10, 11], and are summarized in Tab. 1. The muscle origin/insertion coordinates in Tab. 1 are given with respect to the proximal joint of the related bone.

The model is prepared in MapleSim which allows extensive analytical manipulation of equations of motion which will be discussed later. Such analytical processing speed up the simulations.

Vehicle Dynamics

The vehicle is equally important as the driver, and should be modeled accurately to ensure realistic results. The vehicle model is developed in MapleSim, Fig. 3, and employs a double-wishbone suspension in the front and semi-trailing arm in the rear. A Rack-and-pinion mechanism is used for the steering, and lastly, a Fiala tire model is used to simulate the road/tire interaction.

Driver Model

The driver model in this work is presented as a framework for musculoskeletal analysis of human/vehicle interactions. In humans, the arm motion is controlled by complex commands coming from the Central Nervous System (CNS). The motor control of humans, and in general that of vertebrates, occurs in a dis-

TABLE 1. LIST OF MUSCLE ORIGIN/INSERTION POINTS USED IN THE 3D ARM MODEL

muscle	function	first connection	coordinate (mm)			second connection	coordinates (mm)		
		(origin)	x	y	z	(insertion)	x	y	z
Coracobrachialis (CORB)	SVF	shoulder	20	30	35	humerus	174	20	0
Deltoid (DELT)	SVF	shoulder	-30	40	15	humerus	106	-24	-11
Latissimus dorsi (LAT)	SVE/SAD	shoulder	-35	90	-125	humerus	0	0	-13
Pectoralis major (PECM)	SVF/SHF/SAD	shoulder	45	95	-125	humerus	17	-13	0
Supraspinatus (SUPSP)	SAB	shoulder	-20	90	35	humerus	-14	17	27
Biceps brachii (BIC)	EF	shoulder	0	-15	10	humerus	252	21	0
Triceps brachii (TRIlong)	EE	shoulder	-25	20	-20	radius	38	27	-20
Triceps brachii (TRImed)	EE	humerus	78	11	-10	ulna	38	-27	-15
Brachialis (BRA)	EF	humerus	176	-8	16	radius	33	5	10
Brachioradialis (BRD)	EF	humerus	246	-27	0	radius	283	-12	0

Note - SVF: Shoulder Vertical Flexion; SHF: Shoulder Horizontal Flexion; SAB: Shoulder Abduction; SAD: Shoulder Adduction; EF: Elbow Flexion; EE: Elbow Extension

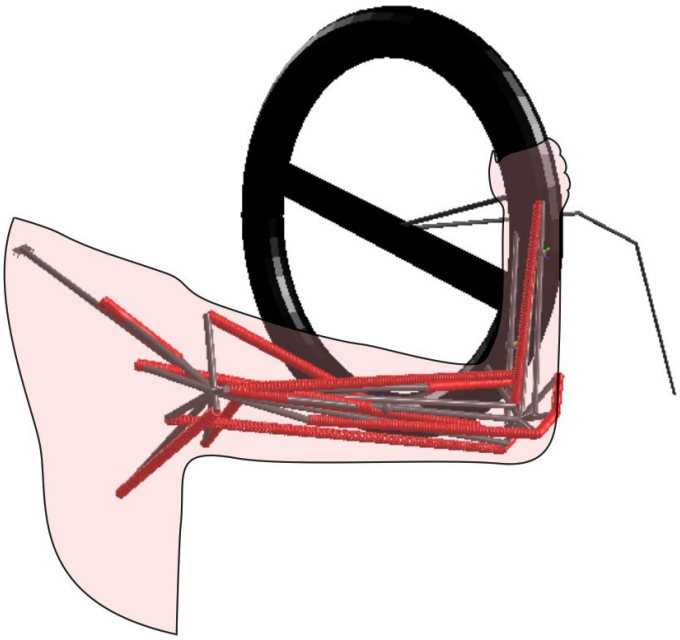

FIGURE 2. THE MUSCLE-ACTUATED ARM MODEL WITH 11 MUSCLES IN MAPLESIM

tributed network – all parts of the CNS including the brain cortex, the cerebellum, and the neural circuits of spinal cord take part in modulating the motor commands. To study the interactions of the musculoskeletal driver model with the vehicle, the complexity of

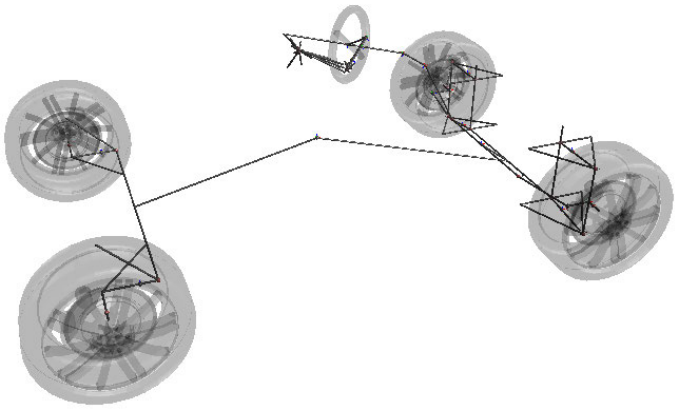

FIGURE 3. VEHICLE AND DRIVER MODEL IN MAPLESIM

the motor control network has to be considered. The schematic of a representative motor control hierarchy is shown in Fig. 4. In this model, the control structure consists of two different layers.

The first layer, the supervisory part, is in the form of a feed-forward/feed-back control scheme. This part estimates the required muscle forces based on the states of the system and a prediction of the future path of the vehicle, and is modeled as a Model Predictive Controller (MPC). The MPC controller decides on the optimal steering wheel angle based on the current state of the system, vehicle dynamics and a short-horizon prediction of the future vehicle path. The cost function that the controller tries to minimize is according to Eqn. 1.

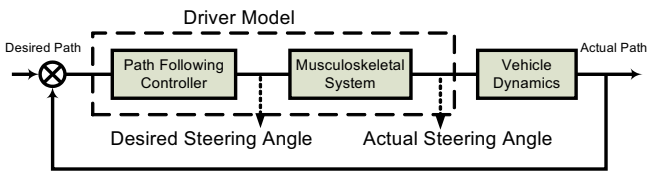

FIGURE 4. WORKFLOW OF THE DRIVER MODEL

$$J_{MPC} = \sum_{i=1}^{P} q\,(y(i) - y_{des}(i))^2 + \sum_{i=1}^{N} r(\theta_{sw}(i))^2 \qquad (1)$$

In Eqn. 1, P and N are the number of prediction and control horizon intervals, respectively. θ_{sw} is the steering wheel angle, and y and y_{des} are vehicle's lateral position and its desired value, respectively. Lastly, q and r are weighting factors in the cost function.

The output of the MPC controller, the steering wheel angle, is then used to calculate the elbow and shoulder joint torques based on the internal dynamics of the arm and the steering system. Finally, muscle forces will be identified from the joint torques using the procedure that will be discussed in the next section.

The second layer of our control hierarchy, the corrective part, provides better control precision and disturbance rejection by means of a feedback control scheme. In human anatomy, the γ-motoneuron activity and stretch reflex are thought to be important mechanisms in improving motion accuracy and attenuating unwanted motions [12, 13]. A disturbance or inaccuracy in the limb position is translated into a deviation of the fascicle length from the desired length [14]. The muscle spindle activity, a nonlinear sum of the muscle length and muscle velocity, changes in accordance with the change in fascicle length. The increase or decrease in the afferent signal from the muscle spindle affects the alpha motoneuron activity, which in turn, increases or decreases the muscle force.

In our model, the stretch reflex is modeled as a proportional-derivative (PD) controller. The input to the PD controller is the deviation of the muscle length from its desired value, which is determined by the MPC controller. Its output represents the afferent signal of the muscle spindle and is added to the reference muscle force to form a mono-synaptic stretch reflex mechanism.

The reflex loop is meant to reduce the effect of disturbance in the system. In this simulation, however, no explicit disturbance is defined. Thus the stretch reflex loop only stabilizes the system by overcoming the disturbance-like numerical issues. However, in future work, the stretch reflex will be of significance in the study of human/steering interfaces [15]. Unexpected road/tire interactions, such as road irregularities, exert disturbances on the system. Moreover, assistive devices such as EPS and lane-keeping will add torque and angle overlay inputs to the steering system, which excite the reflex loops.

Simulation Procedure

The output of the MPC controller is the steering wheel angle. Since the driver/steering wheel is a one-DoF system, the steering wheel angle is enough to solve for all joint angles. Moreover, an inverse dynamic simulation can be performed to find the required steering wheel torque.

knowing the resistive steering wheel torque and joint motion, the joint torques that generate a similar motion in forward dynamic setting can be found. Unfortunately, the calculation of such joint torques is not a trivial problem. The system has only one degree of freedom, and 3 actuators – joint torques at the shoulder and the elbow. To solve for the joint torques a number of assumptions has to be made.

The combination of steering wheel/driver can be described by a set of seven differential-algebraic-equations (DAEs): one differential equation for the steering wheel angle, three differential equations for the three joint angles in the arm, and three algebraic constraint equations:

$$[M] \begin{Bmatrix} \ddot{\boldsymbol{\theta}} \\ \ddot{\theta}_{sw} \end{Bmatrix} + \phi_{\boldsymbol{\theta}}^T \boldsymbol{\lambda} = \begin{Bmatrix} \boldsymbol{T} \\ T_{sw} \end{Bmatrix} \qquad (2)$$

$$\boldsymbol{\phi} = \mathbf{0} \qquad (3)$$

In Eqn. (2), $\boldsymbol{\theta}$ is the 3×1 vector of the joint angles and θ_{sw} is the steering wheel angle. $\boldsymbol{T}$ and T_{sw} are the joint torques and the resistive steering wheel torque, respectively. $\boldsymbol{\lambda}$ is the vector of Lagrange multipliers that represent the reaction forces at the spherical joint. Lastly, $\boldsymbol{\phi}$ and $\phi_{\boldsymbol{\theta}}$ are the constraint equations and the Jacobian matrix, respectively.

If the joint kinematics, from the inverse dynamic simulation, is used in Eqns. (2) and (3), we are remained with 7 algebraic equations. These equations are in terms of four torques ($\boldsymbol{T}$ and T_{sw}) and three reaction forces ($\boldsymbol{\lambda}$). The steering wheel torque is known from the inverse dynamic simulation. In addition, the constraint equations, Eqn. (3), is essentially satisfied when the inverse kinematic motions are used. Therefore, only four independent algebraic equations are left to solve for the six unknowns, $\boldsymbol{T}$ and $\boldsymbol{\lambda}$.

In order to find the joint torques and the reaction forces from the available equations, extra constraints or assumptions have to be made. Our assumption in this case is to minimize the steering column reaction forces, as an index of reducing actuator effort. This is done by employing optimization routines in Matlab. The gradient-based optimization method tries to minimize the reaction forces, while keeping the constraints, Eqn. (2), satisfied.

Even though the solution of the joint torques are based on the equations of motion, there is always numerical error in the solution, which eventually makes the forward dynamic simulation deviate from the reference motion. To compensate for such error, a PID controller is used, which ensures that the system sticks to the reference motion.

The last step in the simulation procedure is the calculation of optimal muscle forces from the joint torques. This can be done by balancing the moments at the joints for the torque- and force-actuated systems. The equations of motion for the muscle-actuated and the torque-actuated arm models are given in Eqn. (4) and Eqn. (5), respectively.

$$[M]\{\ddot{\boldsymbol{\theta}}\}_{3\times 1} = \boldsymbol{g}_1(\boldsymbol{F},\boldsymbol{\theta}) \tag{4}$$

$$[M]\{\ddot{\boldsymbol{\theta}}\}_{3\times 1} = \boldsymbol{g}_2(\boldsymbol{T},\boldsymbol{\theta}) \tag{5}$$

In order to get the same motion from the two systems, the equations of motions of both system should be equal. Thus, by equating the two motions, the relation between the three joint torques and the 11 muscle forces can be found:

$$\begin{aligned} &\boldsymbol{g}_1(\boldsymbol{F},\boldsymbol{\theta}) = \boldsymbol{g}_2(\boldsymbol{T},\boldsymbol{\theta}) \qquad \text{or} \\ &\boldsymbol{G}(\boldsymbol{F},\boldsymbol{T},\boldsymbol{\theta}) = 0 \end{aligned} \tag{6}$$

$\boldsymbol{G}$ in Eqn. (6) (a 3×1 set of functions), relates the 11 muscle forces, $\boldsymbol{F}$, to the three joint torques, $\boldsymbol{T}$, at any given limb position, $\boldsymbol{\theta}$. Therefore the problem of force sharing in this arm has to be solved with a number of assumptions, and in an optimal manner. There are different ways to set up the optimization problem. A common way is to assume the minimization of the following physiological cost function:

$$J = \sum_{i=1}^{11} F_i^2 \tag{7}$$

at each time step, subject to the inequality constraints:

$$0 \le F_i \le F_{i,max} \tag{8}$$

and equality constraints of Eqn. (6) (the values of T and θ_i are known at each time step).

An optimization algorithm can be used to solve for the optimal muscle forces. The computed muscle forces are then used in the forward dynamic simulation of a muscle actuated system.

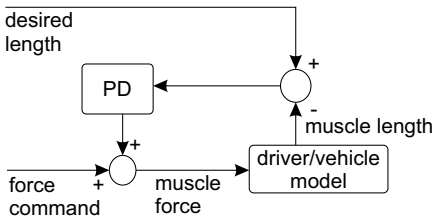

FIGURE 5. THE PD CONTROLLER REALIZATION OF THE STRETCH REFLEX IN THE ARM MODEL

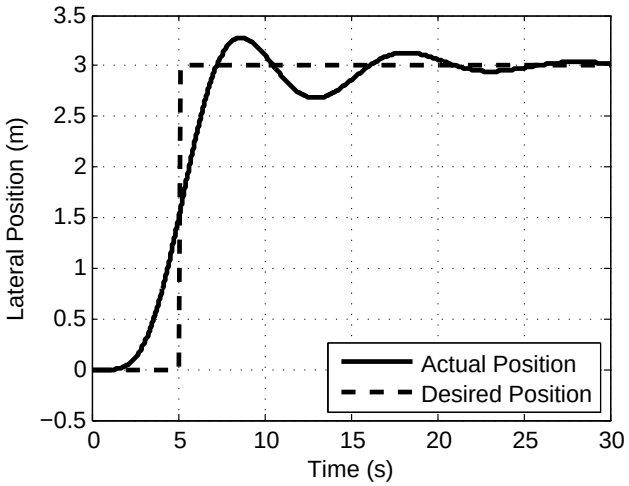

FIGURE 6. VEHICLE LATERAL POSITION

To close the stretch reflex loops, PD controllers are used for each muscle. In PD control loops, the controller input is the error of the muscle length from the desired length, and the correcting output force is added to the previously found optimal muscle force. The schematic of stretch reflex loop is shown in Fig. 5.

SIMULATION RESULTS

All the simulations are done in the Matlab/Simulink environment. The models and optimized simulation code are exported from the MapleSim environment to Matlab.

The simulation results of the model following a step-like lane change at the speed of 6 *m/s* is shown in Fig. 6 and Fig. 7. The MPC controller assigns the steering wheel angle at each time to follow the desired path as closely as possible.

The inverse kinematic simulation results of the vehicle doing a step lane change maneuver provide the angles, angular velocity and acceleration of all joints. Joint angles at shoulder and elbow are shown in Fig. 8, and the computed optimal joint torques are

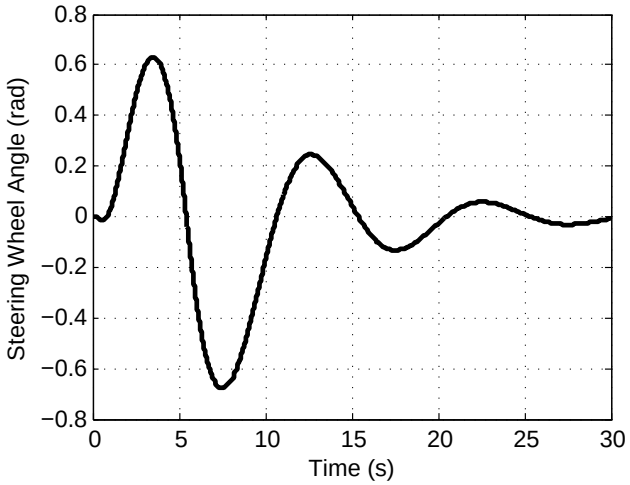

FIGURE 7. STEERING WHEEL ANGLE FROM MPC CONTROLLER

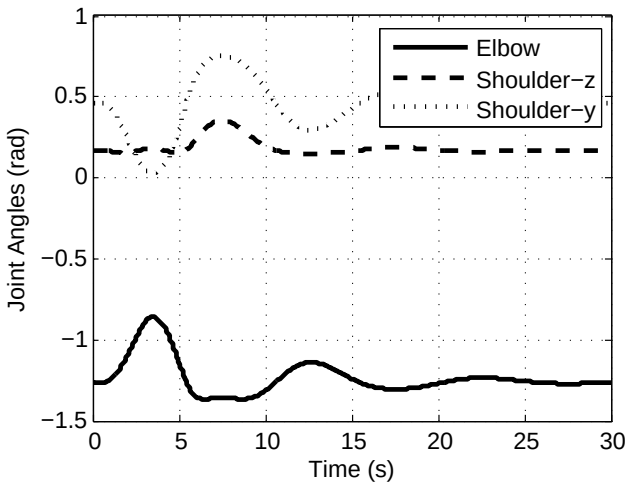

FIGURE 8. 3D ARM JOINT ANGLES

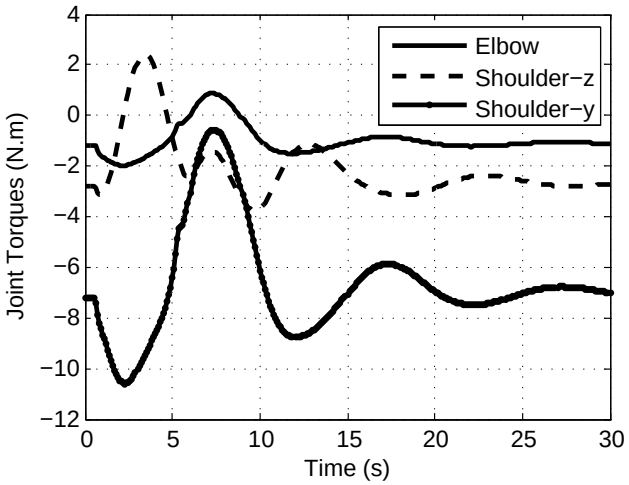

FIGURE 9. JOINT TORQUES FOR THE MANEUVER

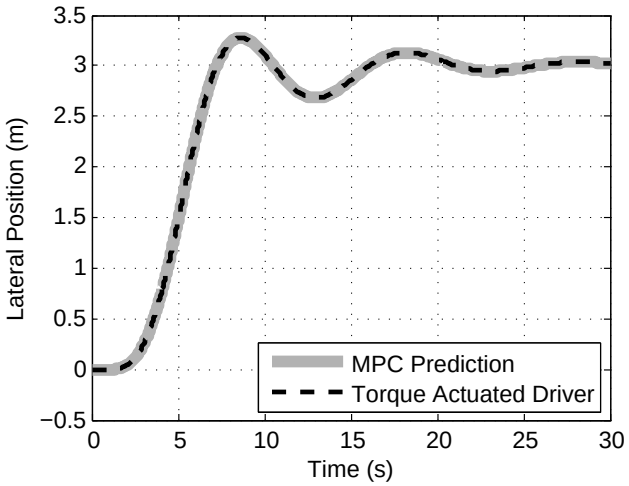

FIGURE 10. VEHICLE PATH IN FORWARD DYNAMIC SIMULATION OF THE TORQUE ACTUATED SYSTEM

shown in Fig. 9.

As can be seen in Fig. 10, the solution of the optimal torques is exact, and if these torques are fed to the arm model again the vehicle follows the same path , therefore validating the joint torque solution.

The optimal muscle forces can be found from the joint torques of Fig. 9 and the method presented in the previous section. The calculated optimal muscle forces are shown in Fig. 11 and Fig. 12. It can be seen that there is no agonist/antagonist co-contraction in elbow muscles. However, shoulder muscles show some co-contraction, which may be due to the 3D nature of the model. Different muscles exert force at different attachment angles; some or all of the muscles have to work together to generate a certain 3D torque. Further investigation has to be done to understand the effect of various assumptions on arm dynamics.

When the calculated optimal muscle forces are used in the forward dynamic simulation of the muscle actuated system, the vehicle follows the path shown in Fig. 6.

CONCLUSIONS

Over the past half-century, many research studies have focused on modeling drivers with different degrees of complexity. Much of the research was focused on predicting the steering

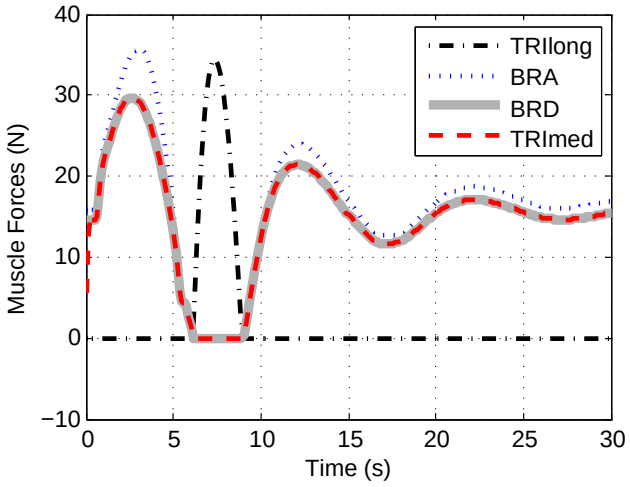

FIGURE 11. OPTIMAL MUSCLE FORCES FOR THE ELBOW MUSCLES

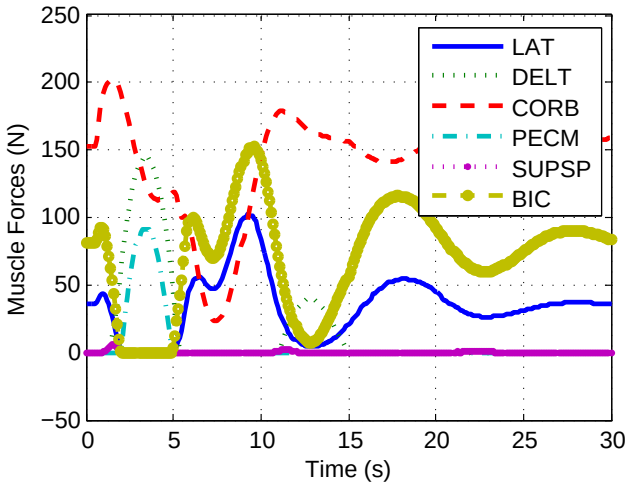

FIGURE 12. OPTIMAL MUSCLE FORCES FOR THE SHOULDER MUSCLES

wheel angle to track a desired vehicle path based on control theories. However, a few research studies concentrated on musculoskeletal dynamics of the driver, which contributes to task performance and disturbance rejection.

In this paper, a hierarchy control approach is selected to perform the motor control. First, a model predictive controller is used to predict the steering wheel angle for a specific maneuver. Then, a three-dimensional model of driver's arm, consisting of a universal joint at the shoulder and a revolute joint at the elbow, actuated with eleven muscles, is developed to perform the predicted motion. Finally, a stretch-reflex is added to each muscle to ensure better control precision and disturbance rejection of the motor control.

Consequently, a three-dimensional neuromuscular driver model in conjunction with a high-fidelity vehicle model is developed to provide both vehicle path planning and arm motions that are physiologically possible. Using this new driver model, we can predict muscle loads and activation signals, which are used to quantify objective criteria such as fatigue and muscle co-contraction for drivers of different age, gender, and physical ability, to learn and understand more about the driver's performance and preferences, and their effect on vehicle control and stability. Finally, this driver model can be used to support the development of new steering technologies such as EPS and lane-keeping.

Future Work

In this paper a framework for studying driver/steering interactions was presented. The models, however, were simplified to expedite the work-flow design process. In the future, the validity of the assumptions for kinematics of the arm, including neglected degrees of freedom and muscles, and the effectiveness of the reflex module will be investigated by human testing. Experiments will identify the required modeling enhancements.

As another future objective, detailed muscle models will be added to the driver model. As a result, alternative criteria such as muscle fatigue and metabolic energy consumption can be considered. The effects of such criteria on muscle co-contraction and steering performance will then be studied.

REFERENCES

[1] Jalali, K., Lambert, S., and McPhee, J., 2012. "Development of a path-following and a speed control driver model for an electric vehicle". *SAE Technical Paper 2012-01-0250*.

[2] Pick, A., and Cole, D., 2003. "Neuro-muscular dynamics and the vehicle steering task". In The Dynamics of Vehicles on Roads and on Tracks, pp. 24–30.

[3] Pick, A., and Cole, D., 2005. "Neuromuscular dynamics in the driver-vehicle system". In 19th IAVSD Symposium.

[4] Cole, D., 2008. "Neuromuscular dynamics and steering feel". In Proceedings of SteeringTech 2008.

[5] Pick, A. J., and Cole, D., 2008. "A mathematical model of driver steering control including neuromuscular dynamics". *Journal of Dynamic Systems, Measurement, and Control,* ***130***(3).

[6] Pick, A. J., and Cole, D., 2006. "Measurement of driver steering torque using electromyography". *Journal of Dynamic Systems, Measurement, and Control,* ***128***(4).

[7] MacAdam, C., 1981. "Application of an optimal preview control for simulation of closed-loop automobile driving". *IEEE Transactions on Systems, Man and Cybernetics 11*.

[8] Mehrabi, N., Sharif, M., and McPhee, J., 2012. "Study of human steering tasks using a neuromuscular driver model". *Advanced Vehicle and Control Conference*.

[9] Maas, R., and Leyendecker, S., 2012. "Optimal control of biomechanical motion using physiologically motivated cost functions". In The 2nd Joint International Conference on Multibody System Dynamics.

[10] Pennestri, E., Stefanelli, R., Valentini, P., and Vita, L., 2007. "Virtual musculo-skeletal model for the biomechanical analysis of the upper limb". *Journal of Biomchanics,* ***40***, pp. 1350–1361.

[11] Gopura, R. A. R. C., Kiguchi, K., and Horikawa, E., 2010. "A study on human upper-limb muscles activities during daily upper-limb motions". *International Journal of Bioelectromagnetism*.

[12] Ackermann, U., 2002. *PAQ Physiology*. McGraw-Hill Europe.

[13] Ting, L. H., van Antwerp, K. W., Scrivens, J. E., McKay, J. L., Welch, T. D. J., Bingham, J. T., and DeWeerth, S. P., 2009. "Neuromechanical tuning of nonlinear postural control dynamics.". *Chaos (Woodbury, N.Y.),* ***19***(2), June, p. 026111.

[14] Hasan, Z., 1983. "A model of spindle afferent response to muscle stretch". *Journal of Neurophysiology,* ***49***(4), pp. 989–1006.

[15] Cole, D., 2012. "A path-following drivervehicle model with neuromuscular dynamics, including measured and simulated responses to a step in steering angle overlay". *Vehicle System Dynamics: International Journal of Vehicle Mechanics and Mobility,* ***50***(4).